Terminal Attachment of Polyethylene Glycol (PEG) Chains to a Gold Electrode Surface. Cyclic Voltammetry Applied to the Quantitative Characterization of the Flexibility of the Attached PEG Chains and of Their Penetration by Mobile PEG Chains

Agnès Anne, Christophe Demaille, and Jacques Moiroux*

Contribution from the Laboratoire d'Electrochimie Moléculaire, Unité Mixte de Recherche Université-CNRS No. 7591, Université de Paris 7 - Denis Diderot, 2 place Jussieu, 75251 Paris Cedex 05, France

Received January 15, 2002

ABSTRACT: In the first part of the study, PEG_{3400}−Fc linear polymeric chains bearing an electrochemically active ferrocene (Fc) head at their loose end are terminally attached at the gold electrode surface. The surface concentration of grafted polymeric chains is measured electrochemically under good solvent (water) conditions, and in the present work, it appears that the electrode is covered with terminally attached PEG chains in the mushroom configuration. The dynamics of the terminally attached chain can be completely characterized according to a model of elastic bounded diffusion which requires the knowledge of the diffusion coefficient D of the loose end and a spring constant, k_{spr}, that is entropic in nature. Both D and k_{spr} are determined. In the second part, the electrode is coated with terminally attached PEG_{3400} and PEG_{20000} chains which are not electrochemically active. The rate constants of penetration and escape of mobile HO−PEG_{3400}−Fc chains in and out of the polymeric coating were determined together with the partition coefficient of HO−PEG_{3400}−Fc between the coating and the surrounding aqueous solution.

Introduction

Heterobifunctional long linear polymeric chains can be terminally attached to various surfaces by only one end provided that this end can react with surface groups to ensure chemical binding, the other end being chemically unreactive with the surface.[1−5]

Depending on the surface concentration of attached polymers, the long chain can exist in two different configurations under good solvent conditions.[6] At low surface concentrations, there is no significant lateral interaction between the terminally grafted chains which exist in the mushroom configuration, whereas the attached polymers exist in the brush configuration at high surface concentration. To obtain stable brushes of terminally attached long linear polymeric chains, the driving force of the grafting must be strong enough to overcome the energy cost of repulsive lateral interaction and stretching of the chains perpendicularly to the surface of attachment.[1,7]

The aim of the present study is 2-fold. In the first part, heterobifunctional linear NHS−PEG_{3400}−Fc molecules made of poly(ethylene glycol) chains of 3400 molecular weight on average (PEG_{3400}) and bearing an *N*-hydroxysuccinimide activated ester (NHS) at one end and a ferrocene (Fc) head at the other[5,8] are terminally attached to the adequately pretreated surface of a planar gold electrode. The NHS activated ester is used for the terminal attachment of the polymer. The loose end of the linear chain bears the Fc head, a redox label that is small and only slightly solvent sensitive.[9] Ferrocene can be reversibly oxidized into ferrocenium (Fc^+) at the gold electrode when the potential of the latter is positive enough. However each Fc head needs to reach the electrode surface to transfer an electron. Therefore, the resulting current may be kinetically controlled by the flexibility of the PEG chain. The excitation and measurement technique used is cyclic voltammetry, and the PEG-modified gold electrodes are analyzed in aqueous solution, a good solvent for PEG chains.[10] At slow enough potential scan rate, all the Fc heads of the grafted layer can be oxidized and the total number of terminally attached PEG−Fc chains can be measured. In the present work, the results gave surface concentrations corresponding to grafted layers made of mushrooms of attached PEG−Fc chains. At high potential scan rate the cyclic voltammograms provide evidence of kinetic control of the current by the PEG chain flexibility, which can then be characterized quantitatively.

In the second part, the electrode surface is covered with mushrooms of terminally attached NHS−PEG chains bearing no Fc heads and cyclic voltammetry is then used to characterize quantitatively the dynamics of penetration of the layer of mushrooms by freely diffusing PEG_{3400}−Fc molecules present in solution. The electrode surface is covered with either terminally attached PEG_{3400} chains or with PEG_{20000} chains, i.e., with PEG chains of markedly different molecular weights (3400 or 20 000).

Experimental Section

Materials. The linear long-chain poly(ethylene glycol) (PEG_{MW}, MW = average molecular weight) derivatives bearing an *N*-hydroxysuccinimide (NHS) active ester at one end and terminated by either a methoxy group at the other end (NHS−PEG_{20000}−OCH_3, (*O*-2-[((*N*-hydroxysuccinimidyl)oxycarbonyl)-ethyl)], *O*′-methylpoly(ethylene glycol) 20 000, average number of O−CH_2CH_2 monomer units, $N \sim 450$), or a biotin (NHS−PEG_{3400}−biotin, (*O*-2-[((*N*-hydroxysuccinimidyl)ethyloxy)carbonyl], *O*′-2-(*N*-biotinamidoethyl)poly(ethylene glycol) 3400, $N \sim 77$) are Shearwater Polymers (Huntsville, AL) reagents. The ferrocene (Fc) end-labeled linear PEG_{3400} chain (HO−PEG_{3400}−Fc, (*O*-[(2-*N*-(β-ferrocenylethylamino)ethyloxycarbonyl]poly-(ethylene glycol)) 3400) and its activated carbonate NHS ester form (NHS−PEG_{3400}−Fc, $N \sim 77$) were synthesized as previously reported.[5] 2-Aminoethanethiol (cysteamine, >98%) and

10.1021/ma020071d CCC: $22.00 © 2002 American Chemical Society
Published on Web 05/24/2002

sodium perchlorate ($NaClO_4$) monohydrate were purchased from Fluka and Merck, respectively. Other chemicals were obtained from commercial sources and were reagent grade or better quality and used as received. All aqueous solutions were made with Milli-Q purified water (Millipore). Phosphate buffer (ionic strength 0.1 M) was made of 49 mM KH_2PO_4, pH adjusted to 7.0 with a 1 M NaOH solution.

Apparatus. Electrochemical experiments were performed with a three-electrode setup using a platinum wire and a KCl saturated calomel electrode (SCE) as the counter and reference electrodes. The reference electrode was separated from the 0.5 M H_2SO_4 or 1 M $NaClO_4$ electrolyte solutions with a bridge terminated with a glass frit, containing respectively an aqueous solution of 0.5 M H_2SO_4 or 1 M NaCl. For potential scan rates v up to 1000 V s^{-1}, the equipment setup was the same as previously described.[8b] For higher scan rate cyclic voltammetry, the signal generator was a Hewlett-Packard 3314A and the curves were recorded with a Tektronix TDS 430A oscilloscope with a minimum acquisition time of 5 ns per point. The potentiostat was the same as previously reported.[11] The temperature in all electrochemical experiments was 25 °C. All cyclic voltammograms were recorded without ohmic drop compensation. Aqueous 1 M $NaClO_4$ was used as the supporting electrolyte solution for electrochemical studies of PEG-modified electrodes.

Pretreatment of the Polycrystalline Gold Electrodes. Gold disk electrodes were constructed by sealing gold wire (125 μm or 1 mm diameter, 99.99%, Goodfellow) within soft glass bodies. The electrodes were polished to mirror finishes using progressively finer grades of alumina polishing suspensions (3, 0.5, and 0.05 μm, Buehler) followed by ultrasonication in water and ethanol. After being dried with an inert gas, the freshly polished electrodes were electrochemically cleaned by cyclic voltammetry between +0.3 and +1.8 V at a potential scan rate of 0.2 V s^{-1} in 0.5 M H_2SO_4 for ~20 cycles. The final anodic scan was stopped in the current minimum region that follows the gold oxidation signal, the electrode potential being held for 5 min at a value of ca. +1.47 V. Under these mild conditions, oxygen is generally assumed to be chemisorbed at gold in a monoatomic layer with a gold oxygen ratio of 1:1.[12] The electrochemical oxidation step was immediately followed by electrochemical reduction of the gold oxide monolayer via a reverse scan at a potential scan rate of 0.2 V s^{-1}. After electrochemical pretreatment the gold electrodes were quickly rinsed with water and ethanol and then immediately used for reaction with cysteamine.

Evaluation of the Effective Surface Area (S_{eff}) of a Gold Disk Electrode of 125 μm Diameter. The S_{eff} surface area was evaluated by integration of the area delimited by the cathodic peak resulting from the reduction of the monolayer of gold oxide (AuO) to gold metal recorded in the final step of the pretreatment procedure (peak potential ~ +0.87 V). The accepted average value of 400 μC/cm^2 for a monolayer of chemisorbed oxygen on polycrystalline gold,[12a,13] was used in this work for the estimation of the effective electrode surface area. We found $S_{eff} = (4.0 \pm 0.5) \times 10^{-4}$ cm^2, which corresponds to a roughness factor of ca. 3.0.

Preparation of PEG-Modified Gold Electrodes. The end-grafting of a monolayer of saturated PEG chains onto the gold surface was typically achieved as follows. In a first step, aminoethylthiol monolayers were formed by immersing the pretreated electrodes in a 20 mM deoxygenated solution of cysteamine ($NH_2-CH_2-CH_2-SH$) in absolute ethanol for 3 h. Following this chemisorption period, the amino-linked gold electrode was removed from the cysteamine solution, thoroughly rinsed with ethanol and water, and washed with phosphate buffer. Terminal covalent attachment of the PEG monolayer was then achieved as follows: a 20 μL droplet of a phosphate buffer solution containing the $NHS-PEG_{MW}$ active ester (concentration ≥ 20 mM) was placed onto the amino modified gold electrode surface in a humid chamber protected from light and left to react for 3−4 h. Prior to electrochemical investigation, the PEG modified gold electrode was washed with water and 1 M aqueous $NaClO_4$ in order to remove thoroughly the PEG chains noncovalently linked to the gold surface.

In control experiments addressing the possibility of immobilization of PEG chains onto cysteamine-coated gold surfaces other than by covalent attachment, $NHS-PEG_{3400}-Fc$ was replaced by its chemically nonreactive form $OH-PEG_{3400}-Fc$.

Optimum Grafting Giving Rise to a Mushroom Configuration. The extent of PEG surface coverage was monitored by means of cyclic voltammetry as described in the text. First of all, we found that a monolayer of terminally attached $PEG_{3400}-Fc$ was rather easily formed by coupling of the amino modified gold surface with an aqueous solution of 20 mM $NHS-PEG_{3400}-Fc$ and that increases in either coupling reaction times (>4 h) or $NHS-PEG_{3400}-Fc$ concentration (up to 100 mM) did not enhance significantly the surface coverage. The saturation surface coverage reached in the present work is 0.1 chain/nm^2, a value close to the highest surface coverage experimentally obtained by other methods of terminal attachment of PEG_{3400} monolayers to various solid surfaces.[2,3] Control experiments indicated that irreversible adsorption of PEG chains onto the amine−gold substrates occurred only to a slight extent: replacing $NHS-PEG_{3400}-Fc$ by its chemically nonreactive form $OH-PEG_{3400}-Fc$ in the immobilization process led to a coverage corresponding to only 5−10% of the mushroom layer. The present saturation coverage indicates that grafted PEG_{3400} chains at the gold surface exist in a coil-like, or mushroom,[6] configuration with the coils being adjacent without significant overlap. It is noteworthy that this maximal surface coverage is reached for a coupling concentration in solution of 20 mM, which corresponds to the critical concentration marking the onset of overlap of PEG_{3400} chains in solution (semidilute regime). Under semidilute conditions, an independence of the surface coverage on the PEG_{3400} coupling concentration similar to the one observed presently has already been reported for the end-grafting of long linear PEG polymeric chains (MW > 2000) to various surfaces.[2,3] A well admitted explanation is that isolated and hydrated PEG molecules actually resist overlap in aqueous solution due to very strong excluded volumes effects.[3b,10b] The resistance to overlap is enhanced when the PEG molecules are linked and confined to a surface. Therefore, only nonoverlapping monolayers are formed by terminal attachment of long PEG chains to solid surfaces, the excluded volume of a long PEG chain being greater than that of a small PEG chain. The semidilute regime for linear PEG_{20000} chains in aqueous solution being reached for a 5 mM concentration, we used coupling solutions of $NHS-PEG_{20000}-OCH_3$ at concentrations ≥5 mM for terminal attachment of $PEG_{20000}-OCH_3$ chains in order to ensure the formation of a saturated monolayer of grafted $PEG_{20000}-OCH_3$ chains in the mushroom configuration.

Compactness of the Grafted Cysteamine Monolayer. The surface concentration of thiol bound to gold was electrochemically assayed in control experiments by a reductive desorption method.[14] The broad voltammetric wave due to reductive stripping of the thiol monolayer bound to polycrystalline gold was recorded at a potential scan rate of 0.2 V s^{-1} in a deaerated solution of 0.1 M NBu_4PF_6 in acetonitrile for a set of cysteamine grafted gold electrodes. Assuming that the reductive desorption of a thiol bound to gold requires one electron,[13,15] integration of the stripping wave gave surface concentrations of grafted cysteamine ranging from 3 to 7 × 10^{-10} mol per cm^2 of effective surface area. Similar values were obtained for dense monolayers of short chain alkanethiolates bound to polycrystalline gold substrates.[14−16] Incidentally, that shows that the surface concentration of amino groups available for PEG attachment is two to four groups per square nanometer of effective surface area, i.e., in large excess (at least 20 times) compared to the surface concentration of PEG long chains, which are actually attached. However, the monolayer of grafted cysteamine, being not very compact, does not block the heterogeneous electron transfer between ferrocene methanol and gold (see text).

Stability of the PEG-Modified Gold Electrodes. The PEG-modified gold electrodes exhibit excellent electrochemical

Chart 1

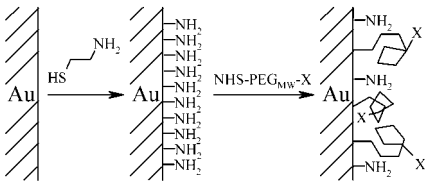

MW = 3400 and X = ferrocene (Fc), or biotin
or MW = 20000 and X = OCH_3

stability in aqueous 1 M $NaClO_4$ electrolyte. In particular, no decrease in the surface coverage of terminally attached $PEG_{3400}-Fc$ was detected after a series of cyclic voltammetry measurements, the investigated potential window extending between − 0.1 and + 0.35 V. When not in use, the electrodes were kept at 4 °C in deaerated water. A typical decrease of ca. 20−30% in the surface coverage was observed after the first overnight storage of ca. 16 h. Beyond the first overnight storage, the PEG-modified gold electrodes exhibit good stability and can be used for a week with no appreciable changes in the electrochemical response.

Results

Terminal Attachment of the PEG Chains to the Surface of the Gold Electrode. As sketched in Chart 1, the gold surface was modified by reaction with cysteamine ($HS-CH_2-CH_2-NH_2$) in a first step under conditions that are described in the Experimental Section. As a consequence, the electrode is covered with superficial amino groups, which are linked to the gold surface. In a second step, the well-established reactivity of the activated NHS ester with superficial amino groups was used for terminal attachment of the PEG chains.[5]

Cyclic Voltammetry at a Gold Electrode Covered with Superficial Amino Groups in the Presence of Mobile $HO-PEG_{3400}-Fc$ Chains Introduced in Solution. At low potential scan rates (v), the observed cyclic voltammetric behavior is as expected for a reversible and Nernstian redox couple, the faradaic current being purely diffusion-controlled. In particular, the difference (ΔE_p) between the anodic and cathodic peak potentials (E_{pa} and E_{pc} respectively) is close to 60 mV and the anodic peak current (i_{pa}) is proportional to $v^{1/2}$.

$$P \underset{}{\overset{E^0_{PQ},\, k_s}{\rightleftharpoons}} Q + e$$

In such circumstances the standard potential (E^0_{PQ}) of the redox couple consisting of the P (=Fc)/Q (=Fc^+) heads is given by $E^0_{PQ} = (E_{pa} + E_{pc})/2$ and $i_{pa} = 0.446FS_gC^0_p(DFv/RT)^{1/2}$, S_g being the geometric electrode surface area, C^0_p the volume concentration introduced of P, and D the diffusion coefficient of the PEG_{3400} chain in solution.[17] We find $D = (1.2 \pm 0.2) \times 10^{-6}$ cm^2/s and $E^0_{PQ} = (140 \pm 5)$ mV/SCE, in agreement with an earlier report,[18] all potentials in the present paper being referred to the KCl saturated calomel electrode (SCE). When $v > 10$ V/s, i_{pa} is still proportional to $v^{1/2}$; however, E_{pa} shifts positively while E_{pc} shifts negatively, revealing that the heterogeneous electron transfer between P/Q and the gold electrode contributes to the kinetic control of the faradaic current.[17] Thus the standard rate constant of heterogeneous electron transfer (k_s) can be deduced from the dependence of ΔE_p on log(v) giving $k_s = (4 \pm 1) \times 10^{-2}$ cm/s.[19]

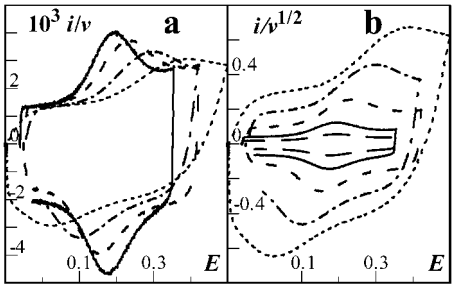

Figure 1. Cyclic voltammograms at various scan rates of a gold disk electrode (125 μm diameter) grafted with terminally attached $PEG_{3400}-Fc$ chains in 1 M $NaClO_4$. The scan rates are: v (in V/s) = 200 (discontinuous lines), v = 944 (continuous lines, superimposed to the previous one in a), v = 4729 (dashed lines), v = 18 887 (dot−dashed lines), v = 48 260 (dotted lines). In part a the current i (in μA) is normalized vs v, in part b, i is normalized vs $v^{1/2}$, the potential E (in V) is referred to SCE, and the temperature is 25 °C.

Cyclic Voltammetry of Mushrooms of Terminally Attached $PEG_{3400}-Fc$ Chains, Which Are Electrochemically Active. The grafting of mushrooms of $PEG_{3400}-Fc$ chains at the gold electrode surface was obtained by reaction of $NHS-PEG_{3400}-Fc$ with the superficial amino groups created at the gold surface as described in the Experimental Section. The cyclic voltammograms recorded at various potential scan rates (v) with a 125 μm electrode bearing terminally attached $PEG_{3400}-Fc$ chains are reproduced in Figure 1.

As can be seen in Figure 1a, symmetric anodic and cathodic peaks are obtained at $v \leq 1000$ V/s, the common value of their peak potentials being 150 ± 10 mV/SCE, i.e., equal to E^0_{PQ} within experimental uncertainty, and the currents coincide with the background currents at potentials much smaller or much greater than E^0_{PQ}. Moreover, the anodic and cathodic faradaic currents are proportional to v at any potential. Such results ascertain that all the Fc heads are allowed to reach the electrode surface and proceed to reversible heterogeneous electron transfer at $v \leq 1000$ V/s; therefore, the total number of terminally attached Fc heads can be derived from the area under either the anodic or cathodic peak, hence the surface concentration Γ of terminally attached $PEG_{3400}-Fc$ chains.[20] Following the procedures giving rise to the maximum surface concentration as detailed in the Experimental Section, we obtained for Γ a maximal value of $(8 \pm 1) \times 10^{-12}$ mol per cm^2 of effective surface area (S_{eff}), measured as described in the Experimental Section. The PEG_{3400} chains contain an average of $N = 77$ monomers of $a = 0.37$ nm size[18,21] and the Flory radius (R_F) for a coil of PEG_{3400} in a good solvent like water is thus $R_F = aN^{3/5} = 5$ nm.[22] If the terminally attached coils do not overlap, each one occupies roughly an area equal to $(R_F)^{2,6}$ a condition that is fulfilled if $\Gamma \leq 7 \times 10^{-12}$ mol/cm^2. The latter value shows that, in the present case, the terminally attached $PEG_{3400}-Fc$ chains exist practically in the mushroom configuration,[6] as sketched in Figure 2.

Above 1000 V/s, the peak-to-peak separation ΔE_p increases with increasing v as reported in Figure 3a while i_{pa} is no longer proportional to v; actually, Figure 3b shows that i_{pa} tends toward a proportionality to $v^{1/2}$ at high v meaning that i_{pa} tends to become diffusion-controlled.[17] Due to the small size of the electrode and the small resistance of the aqueous 1 M $NaClO_4$ solution, the systematic effect of the ohmic drop[17] on the measure of ΔE_p does not exceed the experimental uncertainty represented by the error bars in Figure 3a.

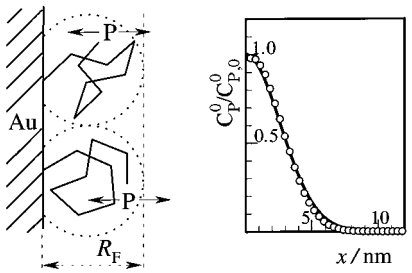

Figure 2. Terminal attachment of PEG_{3400}−Fc chains at the gold surface in the mushroom configuration (with P = Fc): (a) schematic representation of the terminally attached chains;[6] (b) concentration profile giving, at equilibrium, the dependence of the volume concentration of P heads on the distance x measured perpendicularly to the gold surface. The continuous line is given by eq 3, using $k_{spr} = 3k_BT/R_F^2 = 3k_BT/aN^{2\nu}$, with $a = 0.37$ nm and $\nu = 0.58$, while white dots are as given by a self-avoiding walk Monte Carlo simulation (see text).

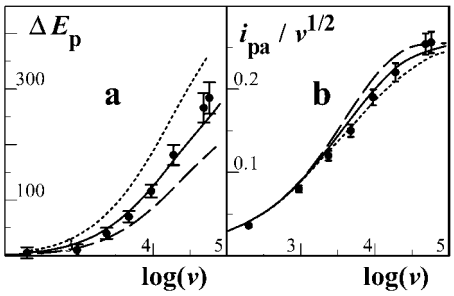

Figure 3. Cyclic voltammetry of a gold disk electrode grafted with terminally attached PEG_{3400}−Fc chains: (a) peak-to-peak separation ΔE_p (in mV) dependence on the scan rate (v in V/s); (b) v dependence of the anodic peak current i_{pa} (in μA), normalized vs $v^{1/2}$. Same experimental conditions as in Figure 1 and means and standard deviations for five different electrodes are given. The continuous lines are computed for the value of the dimensionless parameter $\Lambda^* = 0.4$ (see text); the dotted and dashed lines are computed for $\Lambda^* = 0.2$ and 0.8, respectively.

Cyclic Voltammetry of a Solution of Mobile HO−PEG_{3400}−Fc Chains at Electrodes Grafted with Mushrooms of Terminally Attached and Non Electrochemically Active PEG_{3400} or PEG_{20000} Chains. The grafting of mushrooms of PEG_{3400} or PEG_{20000} non electrochemically active chains at the gold electrode surface was obtained by reaction of NHS−PEG_{3400}−biotin or NHS−PEG_{20000}−OCH_3 with the superficial amino groups created at the gold surface as described in the Experimental Section. The cyclic voltammograms recorded at various potential scan rates in the presence of a solution containing HO−PEG_{3400}−Fc mobile chains are reproduced in Figure 4. Under such conditions, the Fc end of the HO−PEG_{3400}−Fc mobile chain must diffuse toward the electrode and snake through the surface layer of mushrooms to give rise to a faradaic current.

As can be seen in Figure 4, practically identical cyclic voltammograms are obtained at sufficiently slow scan rates with the electrodes bearing terminally attached PEG_{3400} or PEG_{20000} non electrochemically active chains. Moreover, in such a range of scan rates, the electrochemical process is purely controlled by the diffusion of the HO−PEG_{3400}−Fc mobile chains in solution since ΔE_p is ca. 60 mV, $(E_{pa} + E_{pc})/2 = E^0_{PQ}$ and the anodic peak current i_{pa} is proportional to $v^{1/2}$ then purely

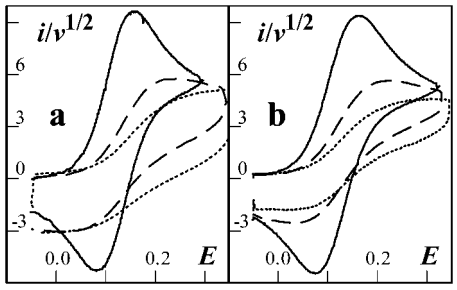

Figure 4. Cyclic voltammograms at various scan rates of a solution of 5 mM HO−PEG_{3400}−Fc mobile chains in 1 M $NaClO_4$ at a gold disk electrode (1 mm diameter) grafted with terminally attached PEG_{3400}−biotin (a) or PEG_{20000}−OCH_3 (b) chains in the mushroom configuration. In part a, the scan rates are v (in V/s) = 0.02 (continuous line), $v = 20$ (discontinuous lines), and $v = 100$ (dotted line). In part b, v (in V/s) = 0.02 (continuous line), $v = 2$ (discontinuous line), and $v = 10$ (dotted line). The current i (in μA) is normalized vs $v^{1/2}$ (in V/s), the potential E (in V) is referred to SCE, and the temperature is 25 °C.

diffusion-controlled.[17] In the following, the anodic peak current expected for such a diffusion-controlled process will be noted $i_{pa,diff}$, i.e., at each v, $i_{pa,diff}$ is calculated so that the ratio $i_{pa,diff}/v^{1/2}$ remains constant and equal to its value determined in the lowest range of v. At high potential scan rates the voltammograms are less and less peak shaped with increasing v, showing that the current is then no longer under pure diffusion control. The threshold at which a change in kinetic control becomes appreciable takes place at much lower v in the case of the PEG_{20000}-grafted electrode than in the case of the PEG_{3400}-grafted electrode. As the voltammograms lose their peak shape with increasing v, an anodic plateau current i_{pl} is measured instead of the anodic peak current i_{pa} and the determination of an anodic peak potential becomes no longer possible. Only the measurement of the potential at mid-wave-height ($E_{1/2,a}$) can be performed accurately. Quantitatively, the dependence of $E_{1/2,a}$ on log(v) is reproduced in Figure 5, parts a and b for PEG_{3400} and PEG_{20000} electrodes respectively, and the dependence of the ratio (i_{pa} or i_{pl})/$i_{pa,diff}$ on log(v) is reproduced in Figure 5, parts a′ and b′. Obviously, $E_{1/2,a}$ increases markedly with increasing v while (i_{pa} or i_{pl})/$i_{pa,diff}$ decreases markedly.

Discussion

Quantitative Analysis of the Dynamics of Mushrooms of PEG_{3400} Chains Terminally Attached to the Electrode Surface. We are interested only in the motion of the P (=Fc) or Q (=Fc^+) heads perpendicular to the electrode surface and we will consequently restrict the formulation of the quantitative analysis of the dynamics of the system to this sole dimension. The parameters we define in the following reflect the net contribution of the processes we consider along the sole direction perpendicular to the electrode surface.

We make use of the model of elastic bounded diffusion we elaborated earlier.[8b] Accordingly, the time (t) and space (x) dependence of the volume concentration (C_P) of P heads is given by a modified form of the second Fick law

$$\partial C_P/\partial t = D[(\partial^2 C_P/\partial x^2) + (k_{spr}D/RT)(\partial x C_P/\partial x)] \quad (1)$$

in which D is the diffusion coefficient of the P head defined by the Einstein relation ($D = k_BT/k_{dr}$ with k_{dr}

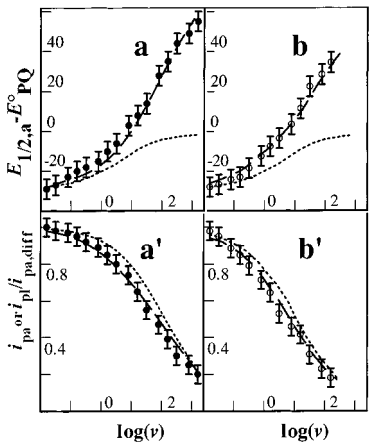

Figure 5. Cyclic voltammetry of a solution of 5 mM HO−PEG_{3400}−Fc mobile chains at a gold disk electrode grafted with terminally attached PEG_{3400}−biotin (black filled scircles) or PEG_{20000}−OCH_3 (white filled circles) chains in the mushroom configuration, potential scan rate v (V/s) dependence of the potential at midpeak or midplateau height $E_{1/2,a}$ (a and b) of the peak (i_{pa}) or plateau (i_{pl}) currents (a′ and b′). The potentials are in mV. i_{pa} and i_{pl} are normalized vs the anodic peak current ($i_{pa,diff}$) obtained at a nongrafted electrode at same v (V/s). Same experimental conditions as in Figure 4 and means and standard deviations are given for three different experiments in which the HO−PEG_{3400}−Fc concentration was C^0_P = 0.4, 2.0, or 5.0 mM. In a and a′, the dotted line is computed for Nernstian heterogeneous electron transfer and $k_{in} = 3 \times 10^{-2}$ cm/s; the dashed line is computed for $k_{in} = 3 \times 10^{-2}$ cm/s and $k_{out}/k_s = 5.0$. In b and b′, the dotted line is computed for Nernstian heterogeneous electron transfer and $k_{in} = 6 \times 10^{-3}$ cm/s; the dashed line is computed for $k_{in} = 6 \times 10^{-3}$ cm/s and $k_{out}/k_s = 1.7$.

the corresponding drag coefficient and k_B the Boltzmann constant), k_{spr} is the spring constant of the rubber elasticity of the PEG chain mimicked by an harmonic oscillator, and x is the spring elongation away from the resting position of the P head. The rubber elasticity is of entropic origin, and $k_{spr} = 3\ k_B T/R_F^2$.[23] In eq 1, k_{spr} is defined as a molar quantity.

The Q volume concentration (C_Q) dependence on t and x is given by an equation analogous to (1). The dynamics of a PEG chain does not depend on whether it bears a P or a Q head; thus, D and k_{spr} are identical for P and Q. Therefore, whatever t,at a given distance perpendicularly to the planar electrode surface:

$$C^0_P = C_P + C_Q \qquad (2)$$

C^0_P being the initial volume concentration given by the equilibrium spatial distribution of fully reduced ferrocene heads at the relevant distance from the electrode surface.

For PEG chains, which are terminally attached to the electrode, the spring elongation perpendicularly to the electrode surface is simply the distance x separating the loose end from surface of attachment located at $x = 0$. The flux $J_{x,t}$ of P at time t through the plane located at a distance x is[8b]

$$J_{x,t} = -D[\partial C_P/\partial x + (k_{spr}/RT)C_P x]$$

At equilibrium, $J_{x,t} = 0$ and $\partial C_P/\partial t = 0$ for any x and t. Taking into account that at $x = 0$, $J_{0,t} = -D(\partial C/\partial x)_{0,t}$ and introducing $C^0_{P,0} = C^0_P$ at $x = 0$, integration then leads to

$$C^0_P = C^0_{P,0} \exp(-k_{spr}x^2/2RT) \qquad (3)$$

Equation 3 shows that, according to model, the concentration profile of the P heads is given, at equilibrium, by a Gaussian distribution (reproduced in Figure 2b) in good agreement with the space distribution of loose chain heads that can be determined by self-avoiding random walk Monte Carlo simulations which gives eq 3′ (see Supporting Information):

$$C^0_{P,i} = C^0_{P,0} \exp[-1.5(i/N^\nu)^2] \qquad (3')$$

with $\nu = 0.58$ and i being an integer ($0 \le i \le N$).

It is also noteworthy to underline that, in the mushroom configuration we consider here, the concentration of the chain heads is maximal at the electrode surface. This contrasts with the case of the brush configuration in which the maximum density of loose chain heads is expected to be located at some distance away from the grafting plane.[24]

The measured surface concentration Γ is related to C^0_P by

$$\Gamma = \int_0^{L_{fs}} C^0_P dx$$

L_{fs} being the length of the fully stretched linear chain.

Thus:

$$C^0_{P,0} = \Gamma\sqrt{\frac{2k_{spr}}{\pi RT}}/erf\left(L_{fs}\sqrt{\frac{k_{spr}}{2RT}}\right)$$

Practically, L_{fs} is long enough ($L_{fs} > 20$ nm) to give

$$C^0_{P,0} = \Gamma\sqrt{\frac{2k_{spr}}{\pi RT}}$$

In the cyclic voltammogram, the faradaic current (i) is proportional to $J_{0,t}$, according to the stoichiometry of the heterogeneous electron transfer between P/Q and the electrode, on one hand, and is kinetically controlled by the potential (E) applied to the electrode according to the Butler−Volmer equation, on the other hand.

$$i = FS_{eff} J_{0,t}$$

and

$$i = FS_{eff}k_s\{C_{P,0} \exp[(\alpha F/RT)(E - E^0_{PQ})] - (C^0_{P,0} - C_{P,0}) \exp[(\alpha - 1)(F/RT)(E - E^0_{PQ})]\}$$

in which α is the transfer coefficient of the heterogeneous electron transfer (α is ca. 0.5) and $C_{P,0}$ the P volume concentration at $x = 0$. Starting from the initial potential (E_i), with $E_i \ll E^0_{PQ}$, the electrode potential E increases linearly with t according to $E = E_i + vt$ during the forward scan until the inversion potential E_{inv} and decreases according to $E = E_{inv} - vt$ back to E_i during the backward scan.

All the preceding equations can be made dimensionless by the following changes in variables and parameters: $y = x\sqrt{Fv/DRT}$, $l = L_{fs}\sqrt{Fv/DRT}$, $\tau = Fvt/RT$, $p = C_P/C^0_{P,0}$ at any y and τ, $\xi = (F/RT)(E - E^0_{PQ})$, $\Lambda = k_s\sqrt{RT/FvD}$, and $\beta = k_{spr}D/Fv$, which compares the experimental observation time RT/Fv to the character-

istic chain motion time $RT/k_{spr}D$, and the dimensionless current $\psi = (i/FS_{eff}C^0_{P,0}\sqrt{FvD/RT})$.

The dimensionless current Ψ is also the dimensionless flux of P at the electrode surface and

$$\Psi = (\partial p/\partial y)_0 = \Lambda \exp(\alpha\xi)[p_0 - (1 - p_0)\exp(-\xi)] \quad (4)$$

The flux $(\partial p/\partial y)_0$ is obtained by integration of the dimensionless form of eq 1

$$\partial p/\partial \tau = \partial^2 p/\partial y^2 + \beta\partial(py)/\partial y \quad (1')$$

with the following initial and boundary conditions:

$$\text{for } \tau = 0 \text{ and } 0 \le y \le l: \quad p = \exp(-\beta y^2/2);$$

for $\tau \ge 0$ and $y = 0$:

$$(\partial p/\partial y)_0 = \Lambda \exp(\alpha\xi)[p_0 - (1 - p_0)\exp(-\xi)]$$

$$\text{for } \tau \ge 0 \text{ and } y = l: \quad p_l = 0 \text{ and } (\partial p/\partial y)_l = 0$$

Obviously, the characteristics of the cyclic voltammogram depend on two parameters only, which are the dimensionless parameters Λ and β, i.e., D and k_{spr} since k_s and α are known. The dimensionless parameter $\Lambda^* = \Lambda/\sqrt{\beta} = (k_s/D)\sqrt{RT/k_{spr}}$ can be used in place of Λ, its physical meaning being more straightforward: Λ^* compares the rate of heterogeneous electron transfer to the rate of motion of the ferrocene head.

At large enough v, the diffusion layer becomes so thin that only the P/Q heads located very close to the electrode surface are given time to move toward the surface and $\beta = 0$, and eq 1′ reduces to the Fick second law for simple diffusion. Then the initial concentration to consider within the restricted volume is the concentration at the immediate vicinity of the electrode $C^0_{P,0}$, and the dimensionless anodic peak current (ψ_{pa}) is $\psi_{pa} = 0.496$.[17] Thus, the corresponding anodic peak (i_{pa}) current is given by

$$\frac{i_{pa}}{\sqrt{v}} = 0.496\sqrt{\alpha}FDC^0_{P,0}\sqrt{\frac{FD}{RT}} = 0.496\sqrt{\alpha}FS_{eff}\sqrt{\frac{FD}{RT}}\sqrt{\frac{2k_{spr}FD}{\pi}}\Gamma$$

and $i_{pa}/\sqrt{v}$ tends to become v independent.

The data reported in Figure 3b shows that then $i_{pa}/\sqrt{v} \rightarrow 0.255 \pm 0.015\ \mu A\ V^{-1/2}\ s^{-1/2}$.

That gives for the response time (t_r) of the system: $t_r = \pi RT/2k_{spr}D = (7 \pm 3) \times 10^{-6}$ s, α, S_{eff}, and Γ being taken as 0.5, 4.0×10^{-4} cm^2 and $(8 \pm 1) \times 10^{-12}$ mol/cm^2 respectively. That gives also $k_{spr}D = (5.4 \pm 2.3) \times 10^8$ J mol^{-1} s^{-1}.

In the general case, ψ_{pa} and the dimensionless anodic and cathodic peak potentials, ξ_{pa} and ξ_{pc} respectively, are obtained by numerical solution of the system of eqs 1′ and 4 taking into account the initial and boundary conditions (see Supporting Information). The product $k_{spr}D$ being then known, β can be calculated for each v, and the theoretical dependence of ΔE_p or $i_{pa}/\sqrt{v}$ on log(v) can be simulated for various values of parameter Λ^*. As can be seen in Figure 3, the computed ΔE_p vs log(v) curve depends more markedly on the value of Λ^* than the $i_{pa}/\sqrt{v}$ vs log(v) curve, and the best fit between the experimental data and the computed variations is obtained for $\Lambda^* = 0.4$. That provides a second relation between k_{spr} and D and enables us to determine k_{spr} and D individually, giving $k_{spr} = 0.20 \pm 0.15$ pN/nm and $D = (5 \pm 3) \times 10^{-8}$ cm^2/s.

The value found for k_{spr} is in good agreement with the experimental value of 0.16 ± 0.09 pN/nm determined for the elasticity of PEG$_{3400}$−Fc chains terminally attached to proteins,[8b] and with the value of 0.5 pN/nm predicted by the entropic origin of k_{spr} ($k_{spr} = 3\ k_BT/R_F^2$).[22]

Quantitative Analysis of the Dynamics of Penetration by Freely Moving HO−PEG$_{3400}$−Fc Chains through Coatings of Non Electrochemically Active PEG$_{3400}$ or PEG$_{20000}$ Terminally Attached to the Electrode Surface. The whole process of permeation of the surface-grafted PEG layer by the freely diffusing redox PEG chains and the ensuing step of heterogeneous electron transfer can be considered as proceeding according to the following reaction scheme:

$$P \underset{k_{out}}{\overset{k_{in}}{\rightleftharpoons}} P_{coating}$$

$$P_{coating} \overset{E^0_{PQ},\ k_s}{\rightleftharpoons} Q_{coating} + e$$

$$Q_{coating} \underset{k_{in}}{\overset{k_{out}}{\rightleftharpoons}} Q$$

P and Q are, respectively, the Fc and Fc$^+$ heads of the freely moving HO−PEG$_{3400}$−Fc (or Fc$^+$) chains, HO−PEG$_{3400}$−Fc being the sole electrochemically active species introduced initially in the solution surrounding the coated electrode at a volume concentration C^0_P The first reaction mentioned in the scheme is equivalent to a partition of P between the solution and the coating film; the third one is equivalent to a partition of Q. Both reactions have the same kinetic (rate constants k_{in} and k_{out} as indicated in the reaction scheme) and thermodynamic characteristics (equilibrium constant $\kappa = k_{in}/k_{out}$) since the partition is essentially controlled by the length of the PEG$_{3400}$ linear polymer.

In dimensionless formulation, if ϵ is the thickness of the coating film and if ϵ_+ and ϵ_- correspond respectively to the solution and the coating sides of the solution/film interface: $p_{\epsilon+} + q_{\epsilon+} = 1$ with $p = C_P/C^0_P$ and $q = C_Q/C^0_P$, C_P and C_Q being the respective volume concentrations of P and Q in solution. The dimensionless current is given by

$$\psi = \frac{i}{FS_gC^0_P\sqrt{FvD/RT}} = \left(\frac{\partial p}{\partial y}\right)_{\epsilon+} = -\left(\frac{\partial q}{\partial y}\right)_{\epsilon+}$$

the dimensionless distance y being defined as indicated earlier in the text.

The dimensionless kinetic parameters are $\Lambda_i = k_{in}\sqrt{RT/FvD}$, $\Lambda_o = k_{out}\sqrt{RT/FvD}$, and Λ, which has already been defined. The equilibrium constant is also given by $\kappa = \Lambda_i/\Lambda_o$, and in the definitions of Λ_i, Λ_o, and Λ, D is the diffusion coefficient of HO−PEG$_{3400}$−Fc in solution that we determined at a gold electrode covered with superficial amino groups, $D = (1.2 \pm 0.2) \times 10^{-6}$ cm^2/s.

The dimensionless equations describing the diffusion/permeation phenomena are as follows.

In solution ($y > \epsilon$), the diffusion of P, or Q, proceeds according to the second Fick law:

$$\frac{\partial p}{\partial \tau} = \frac{\partial^2 p}{\partial y^2} \text{ and } \frac{\partial q}{\partial \tau} = \frac{\partial^2 q}{\partial y^2}$$

At the film solution interface ($y = \epsilon$), the flux balance is expressed by

$$\psi = -(\partial q/\partial y)_{\epsilon+} = \Lambda_o q_{\epsilon-} - \Lambda_i q_{\epsilon+} = (\partial p/\partial y)_{\epsilon+} = -\Lambda_o p_{\epsilon-} + \Lambda_i p_{\epsilon+}$$

meaning that

$$\psi/\Lambda_o = q_{\epsilon-} - \kappa q_{\epsilon+} \quad \text{and} \quad p_{\epsilon-} + q_{\epsilon-} = \kappa$$

After transformation in the Laplace space to linearize the above differential equations and return back to the original space we obtain the following master equation relating the dimensionless current ψ to the dimensionless concentration $q_{\epsilon-}$

$$I\psi + \frac{\psi}{\Lambda_i} = \frac{q_{\epsilon-}}{\kappa} \tag{5}$$

in which $I\psi = (1/\sqrt{\pi}) \int_0^\tau (\psi d\eta/\sqrt{(\tau-\eta)})$, η being an auxiliary variable.

Note that the dimensionless potential ξ and the dimensionless time τ are related since the electrode potential E varies linearly with the time t, $E = E_i + vt$ in the forward scan and $E = E_{inv} - vt$ as already mentioned. The initial and inversion potentials are chosen sufficiently small and great, respectively, to ensure that the characteristics of the cyclic voltammograms do not depend on their values, in particular $\xi \rightarrow -\infty$ for $\tau = 0$.

Compared to the thickness of the diffusion layer, ϵ is so small that $p_{\epsilon-}$ and $q_{\epsilon-}$ are practically equal to the volume concentrations at the electrode surface that depend on the electrode potential. When the heterogeneous electron transfer between the electrode and the P/Q redox couple proceeds at equilibrium, it does not contribute to the kinetic control of the electrochemical response. The heterogeneous electron transfer is then said to be Nernstian and the volume concentrations of P and Q at the electrode surface obey the Nernst law whose dimensionless formulation is $p_{\epsilon-} = q_{\epsilon-}\exp(-\xi)$, ξ being defined as earlier indicated in the text. If it were the case in the present study, then $q_{\epsilon-} = \kappa/[1 + \exp(-\xi)]$ and eq 5 becomes

$$I\psi + \psi/\Lambda_i = 1/[1 + \exp(-\xi)] \tag{6}$$

The fact that a plateau-shaped voltammogram with a plateau height that tends to become v independent is experimentally obtained at high v indicates that in such circumstances Λ_i becomes so small that $I\psi$ can be neglected compared to ψ/Λ_i. Then eq 6 becomes $\psi/\Lambda_i = 1/[1 + \exp(-\xi)]$, and the equation giving the faradaic current is

$$i = FS_g C_P^0 \frac{k_{in}}{1 + \exp[-(F/RT)(E - E_{PQ}^0)]}$$

The rate constant k_{in} can be deduced from the measurement of plateau current $i_{pl} = FSC_P^0 k_{in}$, which is obtained when $E \gg E_{PQ}^0$, and the potential at midplateau height $E_{1/2,a}$ is located at E_{PQ}^0.

When the heterogeneous electron transfer does not proceed at equilibrium the volume concentrations of P and Q are related to the current by the Butler−Volmer equation, whose dimensionless expression is

$$\psi = \Lambda \exp(\alpha\xi)[p_{\epsilon-} - q_{\epsilon-} \exp(-\xi)]$$

or

$$\psi/\Lambda \exp(\alpha\xi) = \kappa - q_{\epsilon-}[1 + \exp(-\xi)]$$

Equation 5 is still valid and, in the original space, that gives

$$q_{\epsilon-} = \kappa (I\psi + \psi/\Lambda_i)$$

and

$$\psi/\kappa\Lambda \exp(\alpha\xi) = 1 - (I\psi + \psi/\Lambda_i)[1 + \exp(-\xi)]$$

or

$$I\psi + (\psi/\Lambda_i)\{1 + (\Lambda_o/\Lambda) \exp(-\alpha\xi)/[1 + \exp(-\xi)]\} = 1/[1 + \exp(-\xi)] \tag{7}$$

It is worth emphasizing that eq 7 is formally equivalent to eq 10a in ref 25 that describes the signal obtained when a redox species diffuses toward a microelectrode array. This illustrates the previously demonstrated equivalence between constrained diffusion toward pinholes and activation controlled permeation of a membrane.[26] Equation 7 can be used to compute the cyclic voltammogram and shows clearly that the latter depends only on Λ_i and on the competition parameter $\Lambda_o/\Lambda = k_{out}/k_s$, which characterizes the competition between the rate of escape of P and Q from the coating and the rate of heterogeneous electron transfer.

When Λ_i is small enough to cause the appearance of a plateau current in the voltammogram and when $\xi \rightarrow \infty$, then $\psi \rightarrow \Lambda_i$ and the same plateau current is obtained as in the case of Nernstian electron transfer. The measurement of the plateau current $i_{pl} = FSC_P^0 k_{in}$ gives the same access to k_{in}. However the potential at midplateau height $E_{1/2,a}$ is no longer located at E_{PQ}^0. As long as $I\psi$ can be neglected compared to ψ/Λ_i, the dimensionless potential at midplateau height $\xi_{1/2a}$ can be deduced from the following equation:

$$\xi_{1/2a} = \ln\{1 + (\Lambda_o/\Lambda) \exp[\xi_{1/2a}(1 - \alpha)]\}$$

Completely irreversible heterogeneous electron transfer would take place when $\Lambda_o/\Lambda \rightarrow \infty$; then $E_{1/2,a}$ would be $E_{1/2,a} = E_{PQ}^0 + (RT/\alpha F) \ln(k_{out}/k_s)$.

In the general case, the cyclic voltammogram can be computed by use of eq 7, which can be solved numerically as explained in Supporting Information. Parts a′ and b′ of Figure 5 show that the peak or plateau current dependence on v is not markedly sensitive to the competition parameter k_{out}/k_s; therefore, it can be used to determine k_{in} without precise knowledge of the competition parameter. On the other hand, parts a and b of Figure 5 show that the dependence on v of the potential at midpeak or midplateau height is quite sensitive to the competition parameter. In a first step k_{in} was deduced from the variation of (i_{pa} or i_{pl})/$i_{pa,diff}$ with log(v) reported in Figure 5, parts a′ and b′. In a second step the competition parameter was adjusted to obtain the best fit of the computed $E_{1/2,a}$ vs log(v)

dependence and the experimentally observed dependence as shown in Figure 5, parts a and b.

For the penetration of the PEG_{3400}−biotin-grafted electrode by HO−PEG_{3400}−Fc mobile chains we found $k_{in} = (3.0 \pm 0.5) \times 10^{-2}$ cm/s and $k_{out}/k_s = 5.0 \pm 0.5$, that gives $k_{out} = (23 \pm 5) \times 10^{-2}$ cm/s since $k_s = (4 \pm 1) \times 10^{-2}$ cm/s and $\kappa = (14 \pm 5) \times 10^{-2}$. For the penetration of the PEG_{20000}−OCH_3-grafted electrode by HO−PEG_{3400}−Fc mobile chains we found $k_{in} = (6 \pm 1) \times 10^{-3}$ cm/s and $k_{out}/k_s = 1.7 \pm 0.2$, that gives $k_{out} = (7.8 \pm 1.8) \times 10^{-2}$ cm/s and $\kappa = (8.5 \pm 3.2) \times 10^{-2}$. Concerning the first case in which the HO−PEG_{3400}−Fc mobile chain must penetrate through a coating of terminally attached PEG_{3400}−biotin chains of identical degree of polymerization in order to reach the electrode surface, it appears that the time response (t_r) of the system is ca. 10^{-5} s since $t_r \approx R_F/k_{in}$, assuming that the average thickness of the coating in the mushroom configuration is ca. $R_F = 5$ nm. That gives a time response, which is close to the time response of 7×10^{-6} s we found for the system consisting of an electrode surface to which PEG_{3400}−Fc chains were terminally attached. Such a result indicates that the elasticity of the HO−PEG_{3400}−Fc chain controls kinetically the response, the insertion of the HO−PEG_{3400}−Fc chain within the grafted coating made of linear polymers of identical average molecular weight proceeding faster. The rate of penetration of the HO−PEG_{3400}−Fc mobile chains through the PEG_{20000}−OCH_3 coating, made of a polymer of significantly higher degree of polymerization, is, as expected, slower than in the preceding case. Actually k_{in} is found to be 5 times smaller.[27] From the thermodynamic point of view, the partition coefficient is roughly halved.

Conclusion

We used cyclic voltammetry as a transient technique to characterize quantitatively the flexibility of terminally attached PEG chains and their penetration by mobile PEG chains. In the first part of the study, PEG_{3400}−Fc linear polymeric chains bearing an electrochemically active ferrocene (Fc) head at one end were terminally attached, at the other end, at the gold electrode surface. The surface concentration of attached Fc heads and thus the surface concentration of grafted polymeric chains can be measured electrochemically. In the present work, they indicate that the electrode is covered with terminally attached PEG chains in the mushroom configuration. The detailed analysis of the electrochemical response confirms that the dynamics of the terminally attached chain can be completely characterized according to a model of elastic bounded diffusion which requires the knowledge of the diffusion coefficient D of the loose end, the one bearing the electrochemically active probe, and a spring constant k_{spr}, entropic in nature. Both D and k_{spr} were determined quantitatively. In the second part the electrode was coated with terminally attached, non electrochemically active, PEG_{3400} and PEG_{20000} chains. Cyclic voltammetry was applied to the quantitative study of the penetration of each type of coating by mobile HO−PEG_{3400}−Fc chains. The rate constants of penetration and escape of the mobile HO−PEG_{3400}−Fc chains in and out of the coating were determined together with the partition coefficient of HO−PEG_{3400}−Fc between the coating and the surrounding solution. It is shown that cyclic voltammetry is a powerful tool for this type of quantitative study provided that the polymeric mobile chain can be labeled with an electrochemically active head.

Supporting Information Available: Text giving details of the self-avoiding random walk Monte Carlo simulation, the numerical solution of eqs 1′ and 4, and the numerical solution of eq 7. This material is available free of charge via the Internet at http://pubs.acs.org.

Note Added after ASAP Posting

This article was released ASAP on 5/24/2002 with an error in the second equation in the right-hand column of the sixth page of the article. The correct version was posted on 5/30/2002.

References and Notes

(1) (a) Auroy, P.; Auvray, L.; Léger, L. *Phys. Rev. Lett.* **1991**, *66*, 719−722. (b) Mir, Y.; Auroy, P.; Auvray, L. *Phys. Rev. Lett.* **1995**, *75*, 2863−2866. (c) Auroy, P.; Auvray, L.; Léger, L. *Macromolecules* **1991**, *24*, 2523−2528. (d) Auroy, P.; Auvray, L.; Léger, L. *Macromolecules* **1991**, *24*, 5158−5166. (e) Auroy, P.; Auvray, L. *Macromolecules* **1996**, *29*, 337−342. (f) Reiter, G.; Auroy, P.; Auvray, L. *Macromolecules* **1996**, *29*, 2150−2157. (g) Bielaski, M.; Rühe, J. *Macromolecules*; **1999**, *32*, 2309−2316. (h) Tran, Y.; Auroy, P.; Lee, L.-T. *Macromolecules*; **1999**, *32*, 8952−8964. (i) Reiter, G.; Sharma, A.; Casoli, A.; David, M.-O.; Khanna, R.; Auroy, P. *Langmuir* **1999**, *15*, 2551−2558.(j) Tran, Y.; Auroy, P. *J. Am. Chem. Soc.* **2001**, *123*, 3644−3654. (k) Casoli, A.; Brendlé, M.; Schultz, J.; Auroy, P.; Reiter, G. *Langmuir* **2001**, *17*, 388−398.

(2) (a) Burns, N. L.; Van Alstine, J. M.; Harris, J. M. *Langmuir* **1995**, *11*, 2768−2776. (b) Emoto, K.; Harris, J. M.; Van Alstine, J. M. *Anal. Chem.* **1996**, *68*, 3751−3757. (c) Emoto, K.; Van Alstine, J. M.; Harris, J. M. *Langmuir* **1998**, *14*, 2722−2729.

(3) (a) Hommel, H.; Halli, A.; Touhami, A.; Legrand, A. P. *Colloids Surf. A.* **1996**, *111*, 67−74. (b) Sofia, S. J.; Premnath, V.; Merill, E. W. *Macromolecules* **1998**, *31*, 5059−5070. (c) Piehler, J.; Brecht, A.; Vialokas, R.; Liedberg, B.; Gauglitz, G. *Biosens. Bioelectron.* **2000**, *15*, 473−481. (d) Lu, H. B.; Campbell, C. T.; Castner, D. G. *Langmuir* **2000**, *16*, 1711−1718. (e) Zhu, X.-Y.; Staarup, D. R.; Major, R. C.; Danielson, S.; Boiadjiev, V.; Gladfelter, W. L.; Bunker, B. C.; Guo, A. *Langmuir* **2001**, *17*, 7798−7803.

(4) Steel, A. B.; Levicky, R. L.; Herne, T. M.; Tarlov, M. J. *Biophys. J.* **2000**, *79*, 975−981.

(5) Anne, A.; Moiroux. J. *Macromolecules* **1999**, *32*, 5829−5835.

(6) de Gennes, P. G. *Macromolecules* **1980**, *13*, 1069−1075.

(7) Zajac, R.; Chakrabarti, A. *Phys. Rev. E.* **1994**, *49*, 3069−3078.

(8) (a) Anne, A. *Tetrahedron Lett.* **1998**, *39*, 561−564. (b) Anne, A.; Demaille, C.; Moiroux, J. *J. Am. Chem. Soc.* **1999**, *121*, 10379−10388.

(9) Hupp, J. T. *Inorg. Chem.* **1990**, *29*, 5010−5012.

(10) (a) Woodley, D. M.; Dam, C.; Lam, H.; LeCave, M.; Devanand, K.; Selser, J. C. *Macromolecules* **1992**, *25*, 5283−5286. (b) Harris, J. M.; Ed. *Poly(ethylene glycol) Chemistry−Biotechnical and Biomedical Applications*; Plenum Press: New York, 1992. (c) Brandrop, J.; Immergut, E. H.; Grulke, E. A. *Polymer Handbook*, 4th ed.; J. Wiley & Sons: New York, 1999. (d) Sukhishvili, S. A.; Chen, Y.; Müller, J. D.; Gratton, E.; Schweizer, K. S.; Granick, S. *Macromolecules* **2002**, *35*, 1776−1784.

(11) Hapiot, P.; Moiroux, J.; Savéant, J.-M. *J. Am. Chem. Soc.* **1990**, *110*, 1337−1343.

(12) (a) Michri, A. A., Pshenichnikov, A. G., Burshtein, R. *Kh. Elecktrokhimya* **1972**, *8*, 364−366. (b) Rand, D. A. J.; Woods, R. *J. Electroanal. Chem.* **1972**, *35*, 209−218.

(13) (a) Cadle, S. H.; Bruckenstein, S. *Anal. Chem.* **1974**, *46*, 16−20. (b) Trasatti, S. Petrii, O. A. *Pure Appl. Chem.* **1991**, *63*, 711−734.

(14) Widrig, C. A.; Chung, C.; Porter, M. D. *J. Electroanal. Chem.* **1991**, *310*, 335−359.

(15) Finklea, H. O. Electrochemistry of Organized Monolayers of Thiols and Related Molecules on Electrodes. In *Electroanalytical Chemistry*; Bard, A. J., Rubinstein, I., Eds.; Marcel Dekker: New York, 1996; Vol. 19, pp 191−368.

(16) Hartwich, G.; Caruana, D. J.; de Lumley-Woodyear, T.; Wu, Y.; Campbell, C. N.; Heller, A. *J. Am. Chem. Soc.* **1999**, *121*, 10803−10812.

(17) Andrieux, C. P.; Savéant, J.-M. Electrochemical reactions. In *Investigations of Rates and Mechanisms of Reactions, Techniques in Chemistry*; Bernasconi, C., Ed., Wiley: New York, 1986; Vol. 6, 4/E, Part 2, pp 305−390.

(18) Demaille, C.; Moiroux, J. *J. Phys. Chem. B.* **1999**, *103*, 9903−9909.
(19) Nicholson, R. S. *Anal. Chem.* **1965**, *37*, 1351−1355.
(20) Laviron, E. Voltammetric Methods for the Study of Adsorbed Species. In *Electroanalytical Chemistry*; Bard, A. J., Ed.; Marcel Dekker: New York, 1982; Vol. 12, pp 53−157.
(21) Kenworthy, A. K.; Hristova, K.; Needham, D.; McIntosh, T. J. *Biophys. J.* **1995**, *68*, 1921−1936.
(22) Flory, P. *Principles of Polymer Chemistry*; Cornell University Press: Ithaca, NY, 1971.
(23) de Gennes, P. G. *Scaling Concepts in Polymer Physics*; Cornell University Press: Ithaca, NY, 1991; pp 29−53.
(24) (a) Cosgrove, T.; Heath, T.; Van Lent, B.; Leermarkers, F.; Scheutjens, J. *Macromolecules* **1987**, *20*, 1692−1696. (b) Milner, S. T.; Witten, T. A.; Cates, M. E. *Europhys. Lett.* **1988**, *5*, 413−418. (c) Milner, S. T.; Witten, T. A.; Cates, M. E. *Macromolecules* **1988**, *21*, 2610−2619. (d) Lai, P.-Y.; Binder, K. *J. Chem. Phys.* **1991**, *95*, 9288−9299. (e) Grest, G.; Murat, M. *Macromolecules* **1993**, *26*, 3108−3117. (f) Lindberg, E.; Elvingston, C. *J. Chem. Phys.* **2001**, *114*, 6343−6352.
(25) Amatore, C.; Savéant, J.-M.; Tessier, D. *J. Electroanal. Chem.* **1983**, *147*, 39−51.
(26) Savéant, J.-M. *J. Electroanal. Chem.* **1991**, *302*, 91−101.
(27) (a) Studies of the exchange process of adsorbed PEG chains on solid supports by freely diffusing PEG chains from aqueous solution can be found in the literature.[27b,c] Among the numerous steps implied in these processes, permeation of the adsorbed layer by incoming coil chains is a potentially rate-limiting step.[27c] It is therefore enlightening to compare the overall exchange rate reported for such systems to the permeation rate we measured in the present work. If we characterize the rate of the early stage of the exchange reaction by an heterogeneous rate constant k_{het}, given by $k_{het} = k_{ex}\Gamma$, k_{ex} being the second-order exchange rate constant and Γ the polymer chain surface concentration, and take the values of $k_{ex} = 100$ cm^3/g s and $\Gamma = 0.35$ mg/m^2 reported for the self-exchange of adsorbed PEG_{10000} chains by their counterpart in solution,[27b] we find $k_{het} = 3.5 \times 10^{-6}$ cm/s. This value is roughly 3 orders of magnitude lower than the value we measured for the permeation rate of a PEG_{20000} mushroom layer by ferrocene-end labeled PEG_{3400} coil chains ($k_{in} = 6 \times 10^{-3}$ cm/s). Although the molecular weight of the incoming polymer chain is higher and the PEG layer structure doubtlessly more compact in the literature work than in our own, the large discrepancy between the two above values does not advocate for a rate-limiting role of the polymer layer permeation by the incoming chains in the kinetics of the exchange process. (b) Mubarekyan, E.; Santore, M. M. *Macromolecules* **2001**, *34*, 4978−4986. (c) Mubarekyan, E.; Santore, M. M. *Macromolecules* **2001**, *34*, 7504−7513.

MA020071D